

Morphometric analysis of axons myelinated during adult life in the mouse superior cervical ganglion

GERALD J. LITTLE AND JOHN W. HEATH

The Neuroscience Group, Faculty of Medicine, The University of Newcastle, New South Wales, Australia

(Accepted 8 November 1993)

ABSTRACT

In experimental studies addressing the regulation of myelin formation and maintenance by Schwann cells, the sympathetic nervous system of young adult rodents has served a key role as an essentially nonmyelinated yet modifiable control tissue. Nevertheless there is clear evidence of substantial myelination in the superior cervical ganglion (SCG) of normal mice and rats of more advanced age. Against this background, interpretation of experimental outcomes in particular sympathetic tissues will require detailed quantitative control data taking account of animal age. To provide a baseline for future investigations on myelin remodelling, an ultrastructural morphometric study of myelinated fibres in the SCG was undertaken in 4 strains (QS, Balb/C, C57 and CBA) of adult male mice aged 32–72 wk. Numbers of myelinated fibres in SCG cross-sections varied substantially between individual animals, and the mean numbers for QS (132), Balb/C (165) and CBA (254) were significantly higher than that for C57 (32). Both axonal and fibre diameter were distributed unimodally (means for the 4 strains ranged from 2.3–2.4 μm and 3.2–3.6 μm respectively). Myelin spiral length was distributed unimodally and skewed to the right (range of means = 227–357 μm) and was significantly greater in QS mice as compared with the other 3 strains. While the mean *g* ratio (axonal diameter/fibre diameter) was significantly lower in QS mice than in the other 3 strains, the range for mean *g* ratio was 0.64–0.73, indicating that myelination had proceeded appropriately even though late in onset in this tissue. The index of circularity was high in all strains, both for axons (range of means = 0.80–0.88) and fibres (range of means = 0.84–0.89). The small axonal and fibre diameter and unimodal distribution are consistent with the characteristics of autonomic myelinated fibres and it is probable that most are postganglionic sympathetic fibres arising within the SCG. In terms of providing a sufficient population of myelinated fibres for future experimental studies, the QS, Balb/C and CBA strains would be preferable to C57 mice.

Key words: Myelin; sympathetic nerve.

INTRODUCTION

Within the rodent sympathetic nervous system, the superior cervical ganglion (SCG) and its preganglionic nerve, the cervical sympathetic trunk, have provided important yet contrasting experimental models in studies focusing on the regulation of myelin formation and maintenance by Schwann cells. In their elegant cross-anastomosis experiments demonstrating that myelination is initiated by axonal signalling, both Aguayo et al. (1976) and Weinberg & Spencer (1976)

utilised the cervical sympathetic trunk as an essentially nonmyelinated nerve trunk. More recently, Voyvodic (1989) used the rat SCG as an essentially nonmyelinated control in studies demonstrating that enlargement of the field of innervation of sympathetic postganglionic neurons triggers myelination of the axons involved. While all these studies were based on young adult animals, it has been shown that a substantial number of postganglionic axons in normal rat SCG do indeed become myelinated during later adult life (Heath, 1983; Kidd et al. 1986; Inuzuka et

al. 1988). It is this population of postganglionic myelinated fibres which becomes involved in the development of 'double myelination', a natural phenomenon occurring both in mouse and rat SCG (Heath, 1982; Kidd & Heath, 1988*a, b*). Experimental manipulation of the double myelination model has demonstrated that axonal contact is not required for ongoing myelin maintenance by Schwann cells in the SCG (Heath et al. 1991; Kidd & Heath, 1991; Kidd et al. 1992) and suggests that myelin breakdown in wallerian degeneration is initiated by some signal arising from the degenerating axon rather than the loss of trophic substances normally supplied by the axon (Heath et al. 1991; Kidd & Heath, 1991; Griffin et al. 1992; Kidd et al. 1992).

These widely varying applications demonstrate the considerable opportunities which sympathetic nerve offers as an experimental model. They also emphasise the importance of detailed control data on numbers of myelinated fibres, and careful selection of animal age, in order to ensure secure interpretations in experiments which may modify the pattern of myelination. In addition, double myelination presents an opportunity to investigate an example of extensive, long-term myelin remodelling, by focusing on the displaced myelin internodes which characterise this model (Kidd & Heath, 1988*b*). In this regard, the mouse SCG offers important practical advantages as an experimental tissue; for example, the prevalence of doubly myelinated regions within the total population of myelinated fibres appears substantially higher than in rat SCG (Heath & Kidd, unpublished). However, little quantitative morphological data are available on any aspect of myelination in mouse sympathetic nerve, and there is no published information on possible strain differences. Therefore, the aims of this study were to document the extent of myelination in normal adult SCG of several common mouse strains, and to establish the morphometric details of myelin internodes not involved in displacement, in order to provide baseline data for a range of future experimental studies.

MATERIALS AND METHODS

Animals and tissue preparation

Thirty seven male mice were used (10 QS, 13 Balb/C:H-2^d, 9 C57Bl/6J:H-2^b and 5 CBA/CaH:H-2^k). All animals were adult, ranging in age from 32–72 wk. While the development of myelin in the mouse SCG is known to occur substantially during adult life (Kidd & Heath, 1988*a*), there is considerable individual

variation in the onset of myelination and in the number of axons which become myelinated. In this study we elected to sample across a broad age range of adult animals; this approach foreshadows future studies of double myelination following experimental interventions, which will require a similar age range.

Under deep pentobarbitone sodium (Nembutal) anaesthesia (90 mg kg⁻¹ i.p.) animals were briefly perfused systemically with 1% sodium nitrite containing heparin (1%) followed by a mixture of 2.5% glutaraldehyde and 2% paraformaldehyde in 0.1 M sodium cacodylate buffer at pH 7.4 (Kidd et al. 1986). The left SCG was dissected free, desheathed and postfixed in buffered 1% osmium tetroxide. Specimens were dehydrated in graded alcohols and embedded in Epon 812 epoxy resin (Probing and Structure, Australia). Thin sections were cut using a Reichert Ultracut E and Diatome diamond knives, mounted on copper grids (300 hexagonal mesh), double stained with uranyl acetate and lead citrate and examined in a JEOL 100CX electron microscope. Analysis was undertaken on complete cross sections of the SCG at a standard level immediately inferior to the origin of the external carotid nerve (Fig. 1).

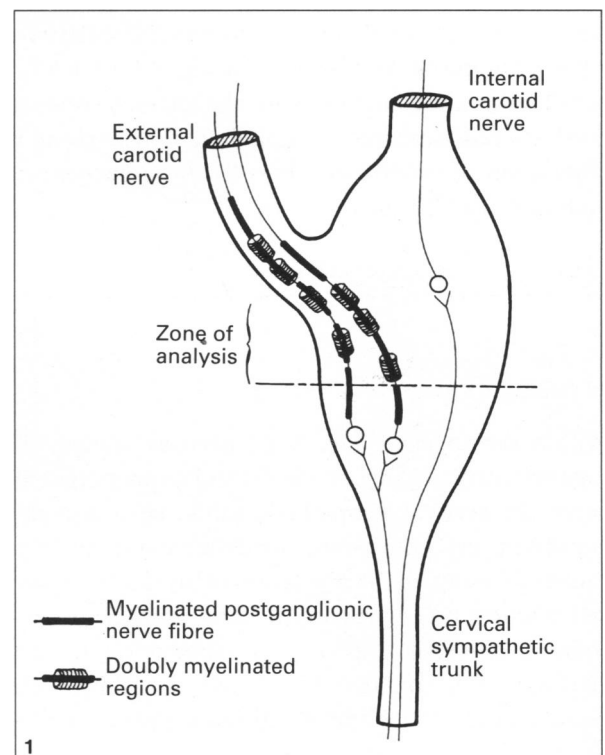


Fig. 1. Diagram of the SCG showing location of standard cross section (zone of analysis) immediately inferior to the external carotid nerve.

Table 1. Number of myelinated fibres (counted by LM) in standard cross-sections of the SCG of individual animals, shown for the 4 mouse strains

Animal	Age*	QS	Age*	Balb/C	Age*	C57	Age*	CBA
1	8	74	8	44	8	18	8	113
2	8	178	8	264	10	52	10	305
3	8	64	8	103	10	11	12	138
4	8	144	10	212	10	39	18	446
5	8	366	10	58	10	11	18	272
6	10	69	10	156	10	43	—	—
7	10	155	10	206	18	38	—	—
8	10	91	10	465	18	39	—	—
9	10	71	10	28	18	37	—	—
10	10	108	10	34	—	—	—	—
11	—	—	12	174	—	—	—	—
12	—	—	18	227	—	—	—	—
13	—	—	18	173	—	—	—	—
Total no. of fibres		1320		2144		288		1274
Mean (CV)**		132.0 (69.39%)		164.9 (72.95%)		32.0 (46.31%)		254.0 (53.23%)

* In months; ** coefficient of variation.

Table 2. Mean number of compact myelin lamellae, and mean axonal and myelinated fibre index of circularity for the 4 mouse strains*

	QS	Balb/C	C57	CBA
Number of lamellae	32.5 (10.1%)	25.2 (14.4%)	21.3 (24.4%)	22.2 (10.6%)
Axonal IC	0.80 (6.0%)	0.88 (5.3%)	0.83 (7.8%)	0.85 (5.3%)
Fibre IC	0.85 (4.1%)	0.89 (3.8%)	0.86 (4.7%)	0.84 (4.8%)

* Bracketed values = coefficient of variation; IC, index of circularity.

Number of myelinated fibres

The total number of myelinated fibres was counted in 0.5 µm toluidine blue-stained sections using a Leitz Ortholux II light microscope equipped with a × 63 oil immersion objective (numerical aperture 1.4). All myelinated profiles were counted; fibres in longitudinal section which appeared to re-enter the section plane were treated as one profile.

Morphometry

All morphometric parameters were determined from electron microscopic images (Bronson et al. 1978). All myelinated fibres in good transverse section were photographed and printed at a final magnification of × 16896. Fibres were judged to be in transverse section by the orientation of axonal microtubules and the definition of the compact myelin lamellae. A further key feature for inclusion of fibres in this

baseline study was maintenance of the typical intimate association between the axon and its investing Schwann cell; in the normal adult SCG this association is disrupted in some internodes by a displacement mechanism culminating in double myelination (Kidd & Heath, 1988*b*). Excluded from analysis were profiles containing Schmidt-Lanterman incisures, nodes of Ranvier, paranodes, myelin whorls and profiles partially obscured by grid bars. Collectively, these stringent criteria led to exclusion of 82% of the total fibre population counted by light microscopy. Data were obtained using a BioQuant IV semiautomatic image analysis system coupled to a digitising tablet (SummaSketch Plus, Connecticut, USA) and an IBM-compatible computer. To obtain accurate calibration of the BioQuant IV system a carbon grating replica (2160 lines/mm) was photographed at the commencement of each EM photographic session, and was used to convert digitised images to real measures (µm). All digitising was performed by one investigator; repeated measures of

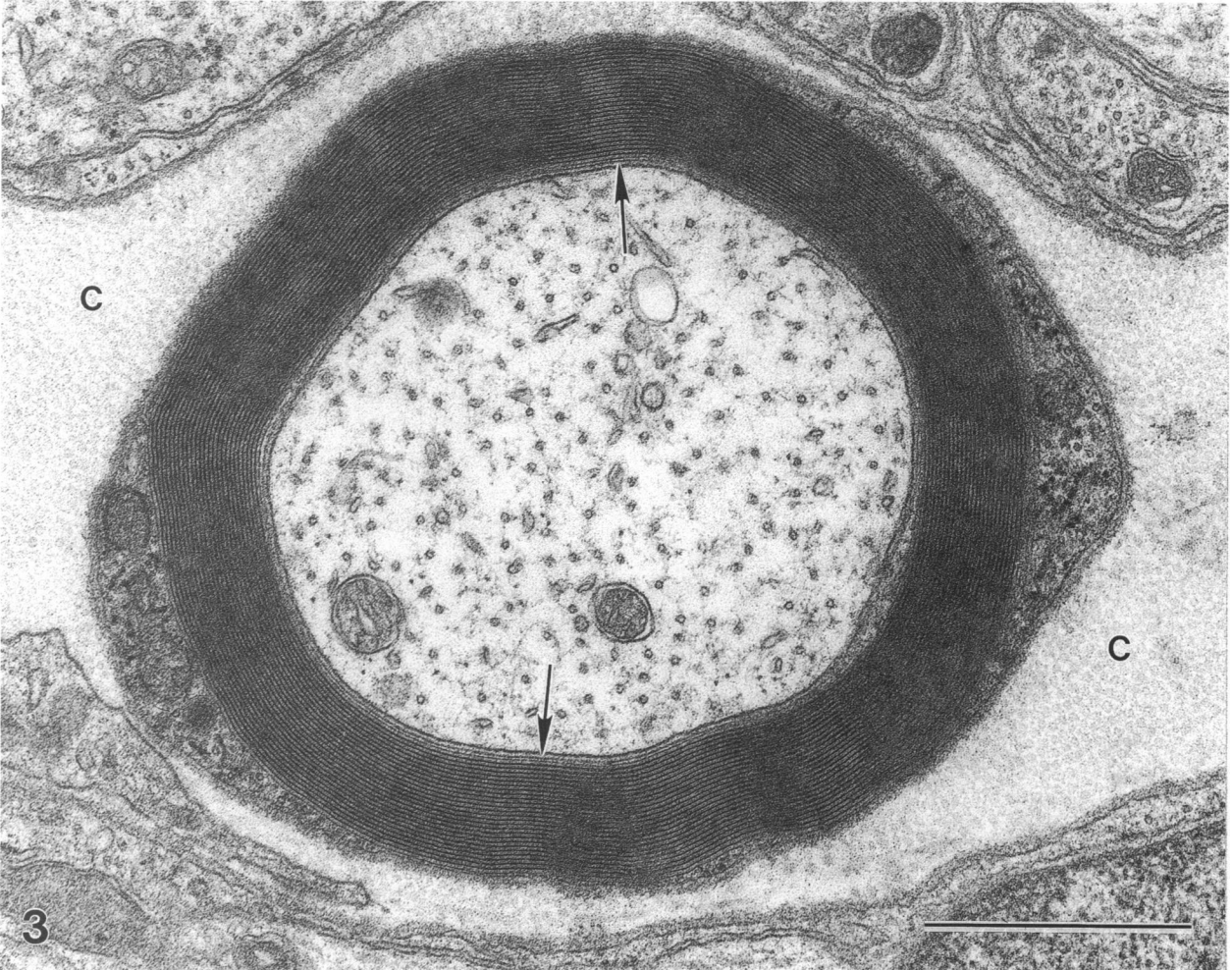
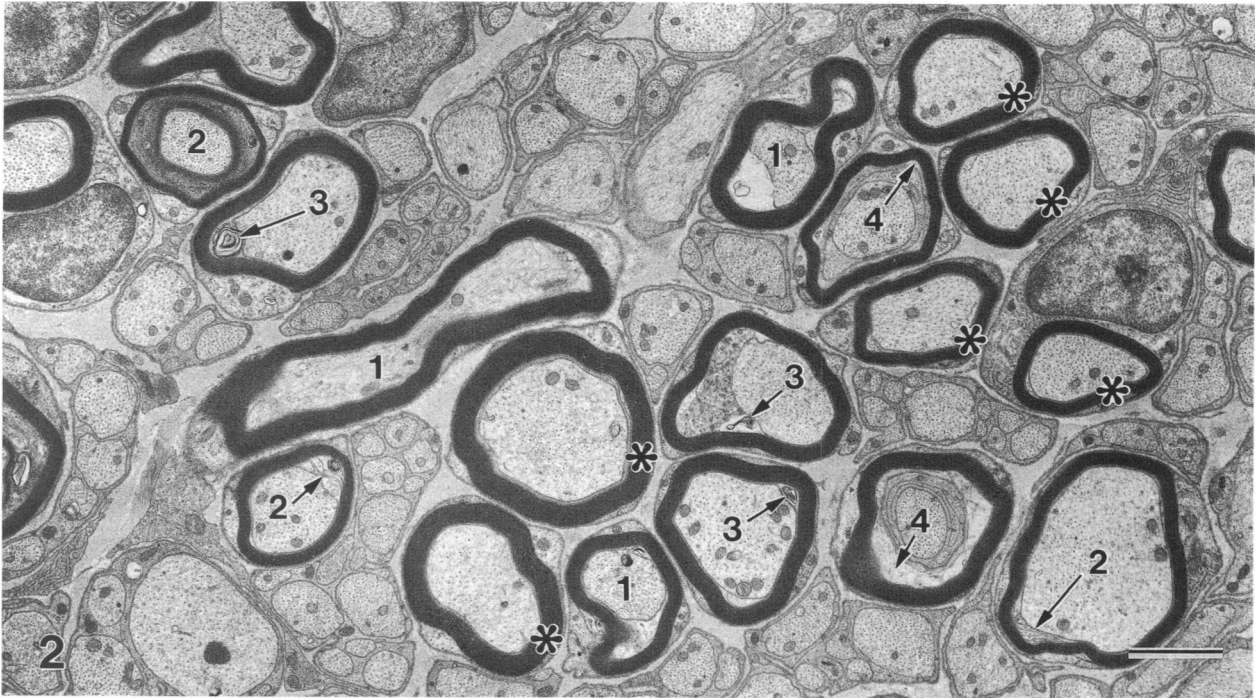


Fig. 2. Low-power electron micrograph of region from standard cross-section of SCG. In this field only those fibres marked with an asterisk were measured. Others were excluded due to inappropriate plane of section (1), the presence of Schmidt-Lanterman incisures (2), focal myelin whorls (3), or displacement of the myelinating Schwann cell from the axon (4) (see Kidd & Heath, 1988b). Bar, 2 μ m.

the same fibre perimeter gave a standard error of 0.004 μm .

In this study, diameters were calculated from area measurements converted to a circular shape; this approach has been demonstrated to provide the best estimate of axonal and fibre diameter in carefully oriented transverse sections of peripheral nerve (Karnes et al. 1977). Axonal area was derived by BioQuant IV from the digitised axon perimeter, and axonal diameter was calculated by the equation:

$$\text{axonal diameter} = 2 \times \sqrt{(\text{axonal area}/\pi)}.$$

Fibre area was derived by BioQuant IV from the digitised outermost major dense line of the compact myelin sheath, and fibre diameter was calculated by the equation:

$$\text{fibre diameter} = 2 \times \sqrt{(\text{fibre area}/\pi)}.$$

The *g* ratio was obtained from the ratio of axonal diameter/fibre diameter.

Myelin spiral length (MSL) was calculated by multiplying the mean myelin perimeter (average of the inner and outer perimeters of the major dense lines) by the number of compact lamellae (counted from each electron micrograph using a binocular microscope) (Friede & Bischhausen, 1980; O'Neill & Gilliatt, 1987). Consequently, the error associated with determining MSL is likely to be approximately twice that found for repeated measure of a single parameter (i.e. S.E.M. \sim 0.008 in total) since the counting of individual myelin lamellae is highly accurate.

The BioQuant IV system calculates a shape factor (index of circularity, IC) using the formula:

$$\text{IC} = 4 \times \pi \times \text{area}/\text{perimeter}^2,$$

where a result of 1 is equivalent to a circle, 0 representing a straight line.

Statistical methods

Statistical comparisons were based on means determined for individual animals. Since some elements of the data appeared not to be normally distributed a nonparametric analysis of variance, the Kruskal–Wallis test, was applied to the data sets. Subsequently the nonparametric Mann–Whitney U-test was used to

further assess differences in parameters (Minitab, Minitab Inc. vs 8.2, 1991). No significant differences relating to age could be demonstrated and animals within each strain were therefore pooled. To assess the distributions of axonal and fibre diameters a bin size of 0.07 μm was chosen, as use of a larger bin size may mask the presence of a bimodal fibre distribution (Guy et al. 1989). Throughout the text, means are quoted with the standard error of the mean (S.E.M.), except in Tables 1 and 2 where the coefficient of variation (CV) is given.

RESULTS

By light microscopy, a total of 5026 myelinated fibres was counted in the standard cross sections. The distribution of these fibres among the strains is shown in Table 1. The Kruskal–Wallis test showed that there was a significant variation in the number of myelinated fibres among strains ($P = 0.0001$). Subsequent Mann–Whitney U-tests showed that the number of myelinated fibres in C57 mice was significantly less than that of the other 3 strains (C57 vs QS, $P = 0.0003$; C57 vs CBA, $P = 0.003$; C57 vs Balb/C, $P = 0.003$; Table 1). Statistically significant differences between the means for Balb/C, QS and CBA mice were not found, reflecting the wide variation in the number of myelinated fibres found among individual animals of all strains.

Figure 2 shows the typical distribution of myelinated fibres in the SCG. By inspection almost all myelinated fibres were small in diameter. The majority of these fibres were located close to the origin of the external carotid nerve, interspersed with greater numbers of unmyelinated fibres. Figure 3 illustrates the quality of preservation on which this quantitative study was based, and shows the narrow periaxonal space typical of myelinated fibres not subject to displacement.

Reflecting the age of the animals some pathological changes were noted in axons at the EM level (minor vacuolation and small aggregations of microfibrils; see also Kidd & Heath, 1988*a*). Small myelin whorls and loops were noted, some apparently degenerative and others reflecting normal folding of the sheath (Fig. 2). Gross changes in the myelin sheath have been described in advanced age (Spencer & Ochoa, 1981;

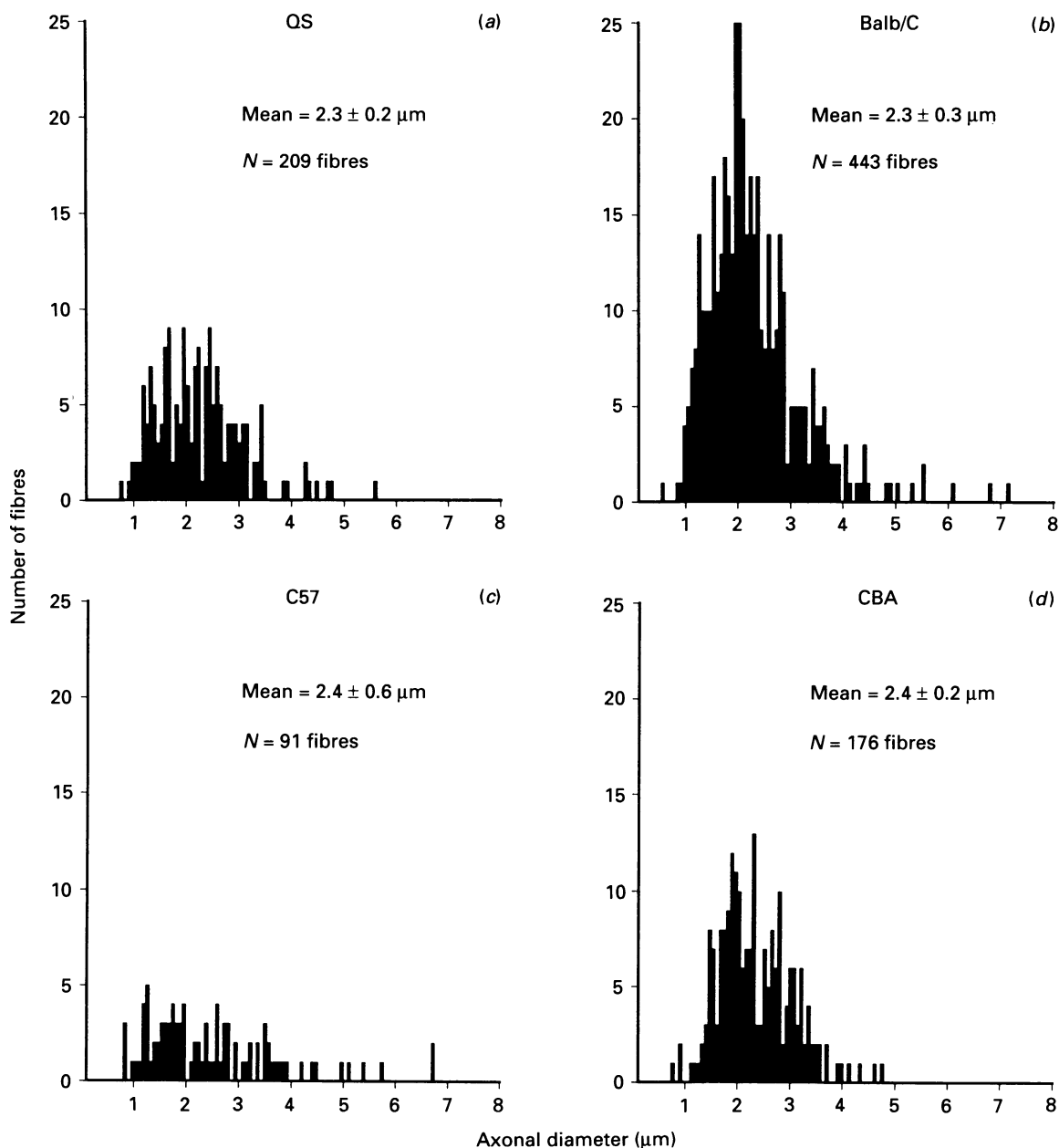


Fig. 4. Histograms of axonal diameter for the 4 strains (a-d). Bin size, 0.07 μm .

Krinke et al. 1988; Knox et al. 1989; Ansved & Larsson, 1990), but were not found in this study.

Stringent application of the acceptance criteria for morphometry resulted in exclusion of the majority of myelinated fibres from this component of the study, due largely to the irregular course of many fibres in this tissue. A total of 919 myelinated fibres was photographed by EM (QS = 209; Balb/C = 443; C57 = 91; CBA = 176).

Histograms of axonal and fibre diameter for the 4 strains are shown in Figures 4 and 5. Both axonal diameter and fibre diameter appeared unimodally distributed, although this is less clear for C57 animals due to the low number of fibres analysed. The mean

axonal diameter ranged from 2.3–2.4 μm , and the Kruskal–Wallis test indicated that there were no significant differences among the strains ($P = 0.94$). Mean fibre diameter ranged from 3.2–3.6 μm , and again the Kruskal–Wallis test showed no significant differences among the strains ($P = 0.37$).

MSL distribution for all strains was unimodal and skewed to the right (Fig. 6). Mean MSL ranged from 227.0–357.2 μm and the Kruskal–Wallis test showed significant differences among the strains ($P = 0.005$). Subsequent Mann–Whitney U-tests showed that the mean MSL in QS mice was significantly greater than that of the other 3 strains (QS vs Balb/C, $P = 0.0007$; QS vs C57, $P = 0.02$; QS vs CBA, $P = 0.006$).

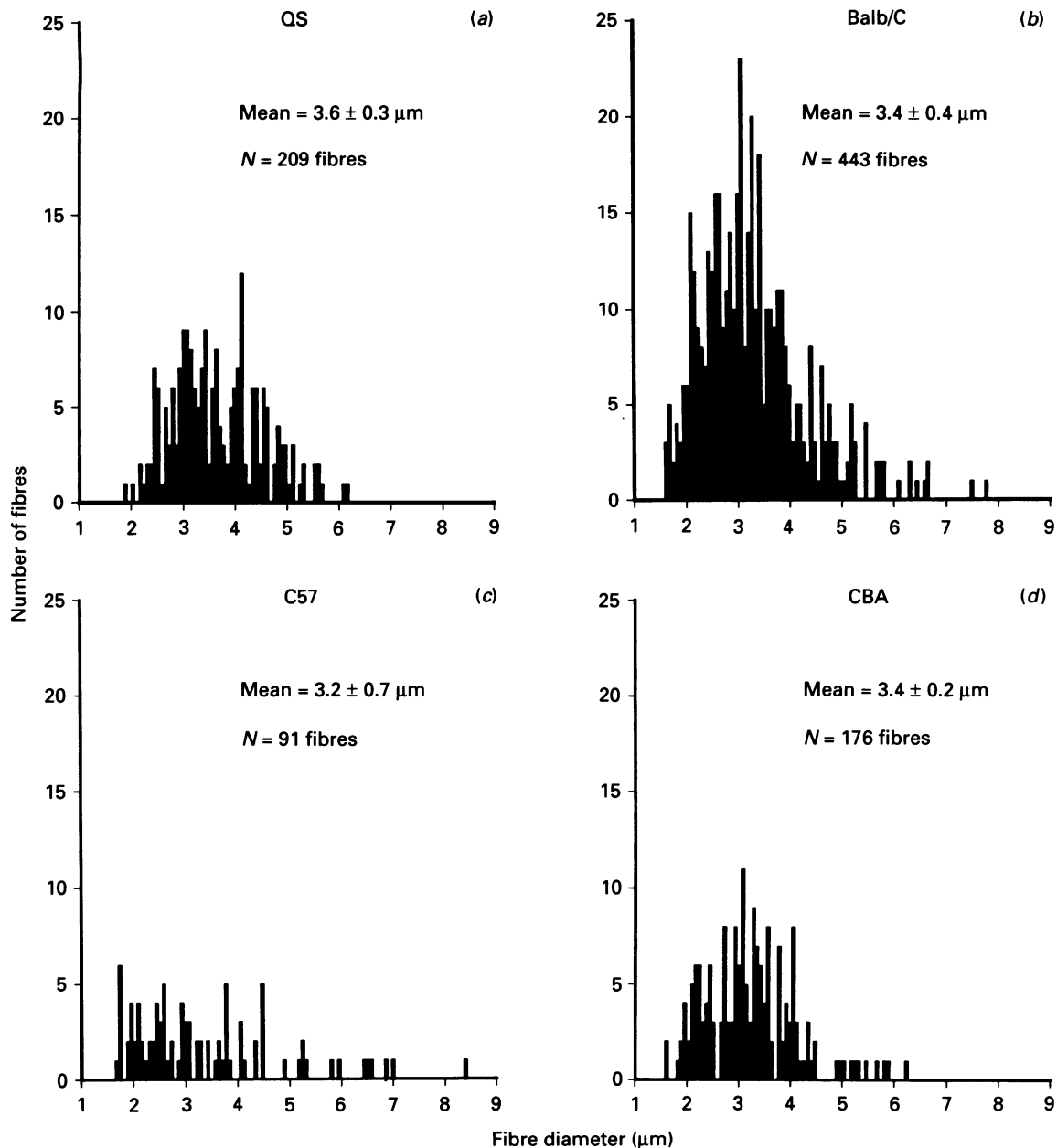


Fig. 5. Histograms of fibre diameter for the 4 strains (a-d). Bin size, 0.07 μm .

Significant differences between mean MSL for Balb/C, C57 and CBA mice were not found. Underlying the calculation of MSL, the Kruskal-Wallis test showed significant variation in the mean number of myelin lamellae among strains ($P = 0.0001$). Subsequent Mann-Whitney U-tests showed that the mean number of compact myelin lamellae was significantly higher in QS mice than in the other strains (Table 2; QS vs Balb/C, $P = 0.0002$; QS vs C57, $P = 0.0001$; QS vs CBA, $P = 0.002$).

Axonal diameter plotted against g ratio for all strains is shown in Figure 7. Mean g ratio varied from 0.64–0.73. The Kruskal-Wallis test indicated significant variation in mean g ratio between the strains

($P = 0.0001$). The mean g ratio for QS mice was significantly smaller compared with the other 3 strains (QS vs Balb/C, $P = 0.005$; QS vs C57, $P = 0.005$; QS vs CBA, $P = 0.004$). In addition, mean g ratio was significantly smaller in Balb/C than in C57 animals ($P = 0.02$).

The mean IC (Table 2) was high in all strains, both for axonal profiles (range 0.80–0.88) and fibre profiles (range 0.84–0.89).

DISCUSSION

This investigation draws attention to the existence of a substantial population of myelinated axons in the

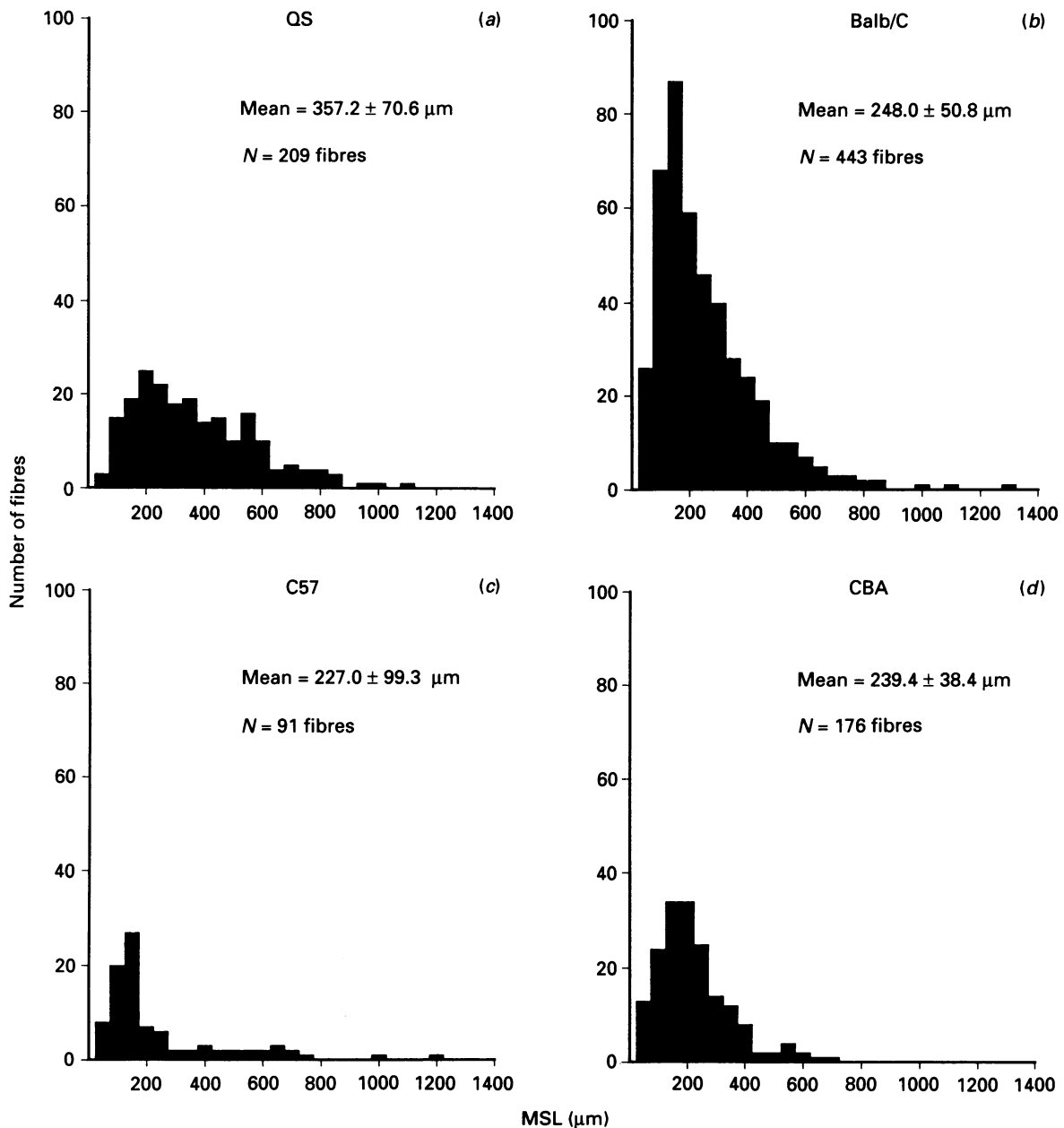


Fig. 6. Histograms of myelin spiral length for the 4 strains (a-d).

SCG of normal adult male mice. In recent years several investigators have elected to use either pre-ganglionic or postganglionic fibres associated with the SCG as 'an essentially nonmyelinated control' in experiments addressing the mechanisms regulating myelination by Schwann cells (Aguayo et al. 1976; Weinberg & Spencer, 1976; Voyvodic, 1989). The conclusions drawn by these workers are not called into question by our present data, since the fibre population we have documented in animals aged 32 wk or more is clearly not present in young animals, as were used by Aguayo et al. (1976), Spencer & Weinberg (1976) and Voyvodic (1989). Nonetheless, our findings demonstrate a natural potential for myelination of axons

within the SCG and external carotid nerve of several mouse strains, and emphasise the importance of age in planning experimental manipulations of myelination in this tissue. The events underlying this late-onset myelination are not known at present, but could involve growth and myelination of new axons, myelination of pre-existing unmyelinated axons consequent upon increased axonal diameter (Voyvodic, 1989), or extension of the region of myelination along fibres with pre-existing partial myelin ensheathment (Inuzuka et al. 1988; Kidd & Heath, 1988b).

A wide variation was found among individual adult animals within all strains, as has been found in the rat (Kidd & Heath, 1988a, b). Nonetheless, significantly

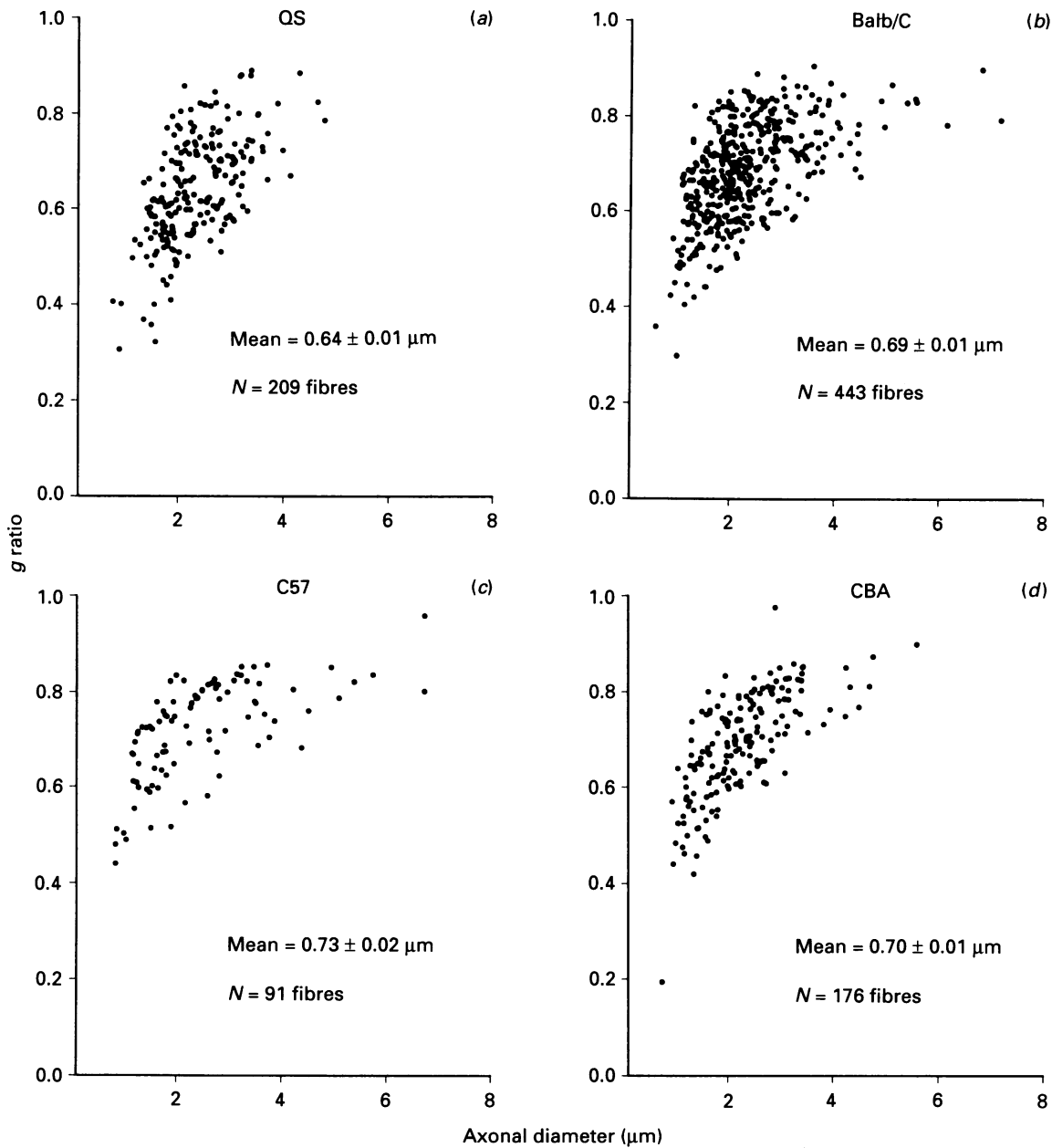


Fig. 7. Plots of g ratio against axonal diameter for the 4 strains (a-d).

fewer myelinated fibres were present in C57 animals when compared with the other 3 strains. Thus in the age range studied, Balb/C, QS and CBA animals would be preferable in terms of availability of an adequate working population for future experimental studies.

Taken together, several observations indicate that the majority of these fibres are postganglionic sympathetic. First, axonal and fibre diameter were small and unimodal, consistent with autonomic myelinated axons. Secondly, in full cross sections of the ganglion, most myelinated axons were located close to the origin of the external carotid nerve (1 of the 2 major postganglionic branches) and within the nerve itself,

with relatively few myelinated fibres distributed elsewhere in the ganglion or in the more inferiorly positioned (preganglionic) cervical sympathetic trunk (see Fig. 1; Little & Heath, unpublished observations). Thirdly, surgical transection of the mouse SCG (at the level used in this study for fibre counts) produces wallerian degeneration in myelinated fibres superior (i.e. distal) to the lesion plane, including those within the external carotid nerve (Kidd & Heath, 1991). Below the lesion plane the effects are those of proximal stump degeneration in the axons and chromatolysis in nerve cell bodies (Kidd & Heath, 1991). A similar population of myelinated fibres present in the SCG of adult rats (Heath, 1983) is largely postganglionic, as

shown by selective surgical and chemical degeneration studies (Heath et al. 1991; Kidd et al. 1992).

In contrast to the numerous reports available for various somatic myelinated nerves, few detailed morphometric studies have been conducted on sympathetic nerve. Our findings for axonal and fibre diameter concur broadly with previous light microscopic reports for human splanchnic nerve (Low et al. 1975*a, b*) and the white rami communicantes associated with human paravertebral sympathetic ganglia (Appenzeller & Ogin, 1973) and an EM study of postganglionic myelination in the rat SCG (Voyvodic, 1989). To the best of our knowledge, our data provide the first report of g ratio and MSL for sympathetic nerve.

Axonal IC for individual mammalian peripheral nerve trunks range from nearly circular values of 0.95 (Knox et al. 1989) to as low as 0.55 (Dockery & Sharma, 1990). Undoubtedly some of these differences reflect the fibre complement of individual nerves (Arbuthnott et al. 1980; Gillespie & Stein, 1983), although methodological variations in tissue preparation and data collection will also contribute (Arbuthnott et al. 1980). In the mouse SCG, mean axonal IC was high in all strains (0.80–0.88). Even so, this estimate is likely to be conservative relative to determination of axonal IC in somatic peripheral nerves, for the reason that internodal length in the mouse SCG is usually less than 50 μm (Kidd & Heath, 1988*b*). Thus in the present study data will have been collected relatively more frequently from a transverse section including the Schwann cell nucleus, which often indents the axon producing a reduced IC at this site (Arbuthnott et al. 1980).

Fibre IC was also high in the SCG (0.84–0.89) and in 3 of the 4 strains was slightly higher than axonal IC. High fibre IC relative to axonal IC was also reported by Gillespie & Stein (1983) for 2 somatic nerves in the cat. These results were found notwithstanding the indenting effect of the Schwann cell nucleus on the myelin sheath (Gillespie & Stein, 1983; this report). It is unlikely that determination of fibre IC was biased by exclusion of fibres containing myelin whorls, since whorls did not appear to be associated particularly with other irregularities in the sheath contour.

The mean MSL for QS mice was significantly greater than that for Balb/C, C57 and CBA animals; this may reflect the combined effect of the following 2 observations. While no statistical differences in fibre diameter were found among the 4 strains, the mean for QS animals was the highest. On the other hand, while no differences in axonal diameter were found among the strains, the mean for QS animals was equal

lowest. While fibre diameter and axonal diameter are each calculated essentially from a single measure, the calculation of MSL is derived from measures both of the outermost and innermost myelin lamellae. It would appear that for QS mice, the combination of the greatest fibre diameter (measured from the outermost myelin lamella) together with the smallest axonal diameter (essentially equivalent to the measurement of the innermost myelin lamella) have resulted in a statistical difference in MSL. This interpretation is supported by direct counting of the compact lamellae in electron micrographs, where QS mice showed a significantly greater mean number of lamellae compared with the other strains (Table 2). Similarly, the statistical difference in mean g ratio for QS mice compared with the other strains probably reflects the combination of greatest fibre diameter and smallest axonal diameter in these animals.

The g ratio is defined as the ratio of axonal diameter to fibre diameter. With regard to optimal conduction velocity, the theoretical optimal value of g is considered to lie in the range 0.6–0.7 (Smith & Koles, 1970), which is in close agreement with the value of 0.6 calculated originally by Rushton (1951). In practice, g varies quite widely, influenced by a range of factors including differences in nerve trunks and among species. For example g ranged from 0.5–0.81 in recent reports on adult somatic nerve by Friede & Beuche (1985*a, b*), Wheeler & Plummer (1989), Fraher et al. (1990), Cavaletti et al. (1992) and Tuisku & Hildebrand (1992). Within individual nerve trunks, g varies with age (Schröder et al. 1978; Friede & Beuche, 1985), region along the axon (Spencer et al. 1973; Fraher et al. 1988) and among the different classes of fibre diameter (Williams & Wendell-Smith, 1971; Fraher et al. 1988, 1990). In small diameter fibres of adult somatic nerves, recent calculations of g varied from a mean of 0.73 in rat ventral root (Fraher et al. 1988) to approximately 0.8 in human sural nerve (Friede & Beuche, 1985*b*). Fraher et al. (1988) also demonstrated a trend for decrease in g with age in small diameter fibres, implying the acquisition of a relatively greater thickness of myelin ensheathment during maturation. While no previous reports of g are available specifically for sympathetic nerve, the mean g values (0.64–0.73) for the 4 mouse strains investigated in this study indicate that myelination has proceeded appropriately in the SCG, even though late in adult life.

This study highlights the presence of substantial numbers of myelinated fibres in the SCG of normal adult mice. In addition, the morphometric data reported will provide a baseline for experimental

approaches provided by the double myelination model. These include the remodelling of a myelin sheath imposed by gradual, long-term displacement from the axon (Kidd & Heath, 1988*a,b*), and the mechanisms involved in the maintenance of myelin internodes which lack axonal contact (Heath et al. 1991; Kidd & Heath, 1991; Kidd et al. 1992).

ACKNOWLEDGEMENTS

Supported by a grant from the National Multiple Sclerosis Society of Australia. We thank Steve Robinson for his excellent technical assistance.

REFERENCES

- AGUAYO AJ, EPPS J, CHARRON L, BRAY GM (1976) Multipotentiality of Schwann cells in cross-anastomosed and grafted myelinated and unmyelinated nerves: quantitative microscopy and radioautography. *Brain Research* **104**, 1–20.
- ANSVED T, LARSSON L (1990) Quantitative and qualitative morphological properties of the soleus motor nerve and the L5 ventral root in young and old rats. *Journal of the Neurological Sciences* **96**, 269–282.
- APPENZELLER O, OGIN G (1973) Myelinated fibres in the human paravertebral sympathetic chain: quantitative studies on white rami communicantes. *Journal of Neurology, Neurosurgery and Psychiatry* **36**, 777–785.
- ARBUTHNOTT ER, BALLARD KJ, BOYD IA, KALU KU (1980) Quantitative study of the non-circularity of myelinated peripheral nerve fibres in the cat. *Journal of Physiology* **308**, 99–123.
- BRONSON RT, BISHOP Y, HEDLEY-WHYTE ET (1978) A contribution to the electron microscopic morphometric analysis of peripheral nerve. *Journal of Comparative Neurology* **178**, 177–186.
- CAVALETTI G, TREDICI G, MARMIROLI P, PETRUCCIOLI MG, BARAJON I, FABBRICA D (1992) Morphometric study of the sensory neuron and peripheral nerve changes induced by chronic cisplatin (DDP) administration in rats. *Acta Neuropathologica (Berlin)* **84**, 364–371.
- DOCKERY P, SHARMA AK (1990) Ultrastructural abnormalities of myelinated fibres in the tibial nerve of streptozotocin-diabetic rats. *Journal of the Neurological Sciences* **98**, 327–345.
- FRAHER JP, KAAR GF, BRISTOL DC, ROSSITER JP (1988) Development of ventral spinal motoneurone fibres: a correlative study of the growth and maturation of central and peripheral segments of large and small fibre classes. *Progress in Neurobiology* **31**, 199–239.
- FRAHER JP, O'LEARY D, MORAN MA, COLE M, KING RHM, THOMAS PK (1990) Relative growth and maturation of axon size and myelin thickness in the tibial nerve of the rat. 1. Normal animals. *Acta Neuropathologica (Berlin)* **79**, 364–374.
- FRIEDE RL, BISCHHAUSEN R (1980) The precise geometry of large internodes. *Journal of the Neurological Sciences* **48**, 367–381.
- FRIEDE RL, BEUCHE W (1985*a*) A new approach toward analyzing peripheral nerve fibre populations. I. Variance in sheath thickness corresponds to different geometric proportions of the internodes. *Journal of Neuropathology and Experimental Neurology* **44**, 60–72.
- FRIEDE RL, BEUCHE W (1985*b*) Combined scatter diagrams of sheath thickness and fibre calibre in human sural nerves: changes with age and neuropathy. *Journal of Neurology, Neurosurgery and Psychiatry* **48**, 749–756.
- GILLESPIE MJ, STEIN RB (1983) The relationship between axon diameter, myelin thickness and conduction velocity during atrophy of mammalian peripheral nerves. *Brain Research* **259**, 41–56.
- GRIFFIN JW, KIDD GJ, TRAPP BD (1992) Interactions between axons and Schwann cells. In *Peripheral Neuropathy*, 3rd edn (ed. P. J. Dyck, P. K. Thomas, J. W. Griffin, P. A. Low & J. F. Poduslo) vol. 1, pp. 317–330. Philadelphia: W. B. Saunders.
- GUY J, ELLIS EA, KELLEY K, HOPE GM (1989) Spectra of G ratio, myelin sheath thickness, and axon and fiber diameter in the guinea pig optic nerve. *Journal of Comparative Neurology* **287**, 446–454.
- HEATH JW (1982) Double myelination of axons in the sympathetic nervous system. *Journal of Neurocytology* **11**, 249–262.
- HEATH JW (1983) The sympathetic nervous system: a novel perspective on the control of myelinating Schwann cells. In *Molecular Pathology of Nerve and Muscle* (ed. A. D. Kidman, J. K. Tomkins, C. A. Morris & N. A. Cooper) pp. 21–37. Clifton, New Jersey: Humana Press.
- HEATH JW, KIDD GJ, TRAPP BD, DUNKLEY PR (1991) Myelin maintenance by Schwann cells in the absence of axons. *Neuroscience Letters* **128**, 277–280.
- INUZUKA T, QUARLES RH, TRAPP BD, HEATH JW (1988) Analysis of myelin proteins in sympathetic peripheral nerve of adult rats. *Developmental Brain Research* **38**, 191–199.
- KARNES JL, ROBB R, O'BRIEN PC, LAMBERT EH, DYCK PJ (1977) Computerized image recognition for morphometry of nerve attribute of shape of sampled transverse sections of myelinated fibers which best estimates their average diameter. *Journal of the Neurological Sciences* **34**, 43–51.
- KIDD GJ, HEATH JW, DUNKLEY PR (1986) Degeneration of myelinated sympathetic nerve fibres following treatment with guanethidine. *Journal of Neurocytology* **15**, 561–572.
- KIDD GJ, HEATH JW (1988*a*) Double myelination of axons in the sympathetic nervous system of the mouse. I Ultrastructural features and distribution. *Journal of Neurocytology* **17**, 245–261.
- KIDD GJ, HEATH JW (1988*b*) Double myelination of axons in the sympathetic nervous system. II. Mechanisms of formation. *Journal of Neurocytology* **17**, 263–276.
- KIDD GJ, HEATH JW (1991) Myelin sheath survival following axonal degeneration in doubly myelinated nerve fibers. *Journal of Neuroscience* **11**, 4003–4014.
- KIDD GJ, HEATH JW, TRAPP BD, DUNKLEY PR (1992) Myelin sheath survival after guanethidine-induced axonal degeneration. *Journal of Cell Biology* **116**, 395–403.
- KNOX CA, KOKMEN E, DYCK PJ (1989) Morphometric alteration of rat myelinated fibers with aging. *Journal of Neuropathology and Experimental Neurology* **48**, 119–139.
- KRINKE G, FROELICH E, HERRMANN M, SCHNIDER K, DASILVA F, SUTER J, TRABER K (1988) Adjustment of the myelin sheath to axonal atrophy in the rat spinal root by the formation of infolded myelin loops. *Acta Anatomica* **131**, 182–187.
- LOW PA, WALSH JC, HUANG CY, MCLEOD JG (1975*a*) The sympathetic nervous system in alcoholic neuropathy. A clinical and pathological study. *Brain* **98**, 357–364.
- LOW PA, WALSH JC, HUANG CY, MCLEOD JG (1975*b*) The sympathetic nervous system in diabetic neuropathy. A clinical and pathological study. *Brain* **98**, 341–356.
- O'NEILL JH, GILLIATT RW (1987) Adaptation of the myelin sheath during axonal atrophy. *Acta Neuropathologica (Berlin)* **74**, 62–66.
- RUSHTON WAH (1951) A theory of the effects of fibre size in medullated nerve. *Journal of Physiology* **115**, 101–122.
- SCHRÖDER JM, BOHL J, BRODDA K (1978) Changes in the ratio between myelin thickness and axon diameter in the human developing sural nerve. *Acta Neuropathologica (Berlin)* **43**, 169–178.
- SMITH RS, KOLES ZJ (1970) Myelinated nerve fibres: computed

- effect of myelin thickness on conduction velocity. *American Journal of Physiology* **219**, 1256–1258.
- SPENCER PS, RAINE CS, WIŚNIEWSKI H (1973) Axon diameter and myelin thickness – unusual relationships in dorsal root ganglia. *Anatomical Record* **176**, 225–244.
- SPENCER PS, OCHOA J (1981) The mammalian peripheral nervous system in old age. In *Ageing and Cell Structure* (ed. J. E. Johnson Jr.) pp. 35–103. New York: Plenum.
- TUISKU F, HILDEBRAND C (1992) Nodes of Ranvier and myelin sheath dimensions along exceptionally thin myelinated vertebrate PNS axons. *Journal of Neurocytology* **21**, 796–806.
- VOYVODIC JT (1989) Target size regulates calibre and myelination of sympathetic axons. *Nature* **342**, 430–433.
- WEINBERG HJ, SPENCER PS (1976) Studies on the control of myelinogenesis. II. Evidence for neuronal regulation of myelin production. *Brain Research* **113**, 363–378.
- WHEELER SJ, PLUMMER JM (1989) Age-related changes in the fibre composition of equine peripheral nerve. *Journal of the Neurological Sciences* **90**, 53–66.
- WILLIAMS PL, WENDELL-SMITH CP (1971) Some additional parametric variations between peripheral nerve fibre populations. *Journal of Anatomy* **109**, 505–526.